Braz J Phys (2014) 44:55–63
DOI 10.1007/s13538-013-0160-z

NUCLEAR PHYSICS

Study of Different Forms of Density Distributions in Proton–Nucleus Total Reaction Cross Section and the Effect of Phase in NN Amplitude

M. A. Alvi

Received: 27 February 2013 / Published online: 2 October 2013

Abstract Proton total-reaction cross-section (σ_R), measurements for about five nuclei in the range ^{12}C to ^{208}Pb at beam energies spanning 40–800 MeV have been analyzed in a systematic way by using the optical limit approximation of the Coulomb-modified Glauber multiple scattering theory. Two different phenomenological nuclear density distributions of the target nucleus in addition to the realistic one have been used in the present analysis. By applying the energy dependence in the slope parameter of nucleon–nucleon (*NN*) scattering amplitude, it is found that in general, the predictions of σ_R with the phenomenological Gambhir and Patil density distribution agree fairly well with the experimental data. The inclusion of phase in the *NN* amplitude improves the theoretical results. Our analysis shows that the calculated total reaction cross sections closely reproduce the measured data over the whole range of energy considered in this work. To validate our analyses, we have also obtained a fairly good representation of elastic p-nucleus differential scattering cross section data. The effect of a Coulomb energy shift in the proton beam has also been studied.

Keywords Coulomb-modified Glauber model · Optical limit approximation · Phase variation of *NN* amplitude · Folded-Yukawa density · Coulomb shift in beam energy

1 Introduction

Nucleon–nucleus integrated cross sections constitute a key observable in fundamental nuclear research as well as in the applications of nucleon-induced reactions. The total reaction cross section σ_R is of particular importance in nuclear technology such as nuclear waste treatment, safety assessment, nuclear transmutation, and medical therapy. From the fundamental point of view, its description within microscopic approaches constitutes a test to the understanding of the physics involved in the interaction and provides us some important information such as the size of nucleus, nuclear structure, and density distribution of nucleons in the nucleus. Apart from its application, with the advent of radioactive ion-beam technique, the interest in the measurement of σ_R is revitalized to study the structure of nuclei even far from the valley of stability [1–5].

For several years, extensive analyses of proton reaction cross sections have been performed in a wide range of energies and mass numbers. In most of these analyses, generally, the effort is devoted to the determination of either general parameterizations of σ_R [6–10] or global nucleon optical potential [6, 11–14]. In recent years, Glauber multiple scattering model [15] has also been applied to study the energy and mass dependence of proton reaction cross sections. Initially, the Glauber model was indeed designed for high-energy approximation. However, it was found to work fairly well, for both the nucleus–nucleus reaction cross section and the differential elastic scattering cross sections, over a broad energy range [16–22] i.e., the model reproduced the results at incident energies well down to about 20 MeV/nucleon. Thus, for including the low-energy effects of increasing the nucleon–nucleon (*NN*) interaction, the above stated original Glauber model has been modified to take care of the finite range effects [23–25] in profile function and the Coulomb-modified trajectories. Alvi [26] has applied the Coulomb-modified Glauber model to derive an analytical expression for proton reaction cross section. Using an approximate form for the Helm model form factor for

M. A. Alvi (✉)
Department of Physics, Faculty of Science, King Abdulaziz University, Jeddah 21589, Saudi Arabia
e-mail: alveema@hotmail.com

the distribution of nucleons in nuclei, the proposed analytical expression [26] reproduces nicely the proton σ_R data at energies spanning 20–860 MeV.

In the calculation of total reaction cross section σ_R, one of the basic inputs in the Glauber model calculations is the *NN* scattering amplitude $f_{NN}(q)$, defined as $f_{NN}(q) = \frac{ik\sigma_{NN}}{4\pi}(1-i\alpha_{NN})e^{-a_{NN}q^2/2}$. The parameters *NN* total cross section σ_{NN}, and the ratio of the real to the imaginary parts of the forward scattering amplitude α_{NN}, are quite rightly obtained from *NN* scattering experiments using the phase shift solutions and dispersion relations [27]. The parameter a_{nn} in $\exp(-a_{nn}q^2/2)$, known as the slope parameter, can also be determined with a fair degree of certainty at high energies. But at low-intermediate energies, it has been discussed in great detail in Ref. [28] that for a_{nn}, many different values ranging from zero to $1.24 fm^2$ have been assumed even at the same energy to get a satisfactory fit to the experimental nucleus–nucleus elastic differential scattering data. For example, Lenzi et al. [18] have used $a_{nn}=0$ for nucleon energies up to 120 MeV and $a_{nn}=0.02 fm^2$ at energy 200 MeV. Chiragi and Gupta [19, 20] treated it as an adjustable parameter, Ray [27] has used $a_{nn}=1.02$ to $1.24 fm^2$ at different energies, and El-Gogary et al. [29] have used $a_{nn}=0.54$ and $0.51 fm^2$ at energies 45 and 200 MeV/nucleon, respectively. At energies below 300 MeV, Ogawa et al. [30] have calculated it by setting the total elastic *NN* cross section equal to the *NN* total cross section. The parameter a_{nn} is an energy-dependent quantity; unfortunately, no known good phenomenological parameterization has ever been discussed in the literature.

Franco and Yin [31] had earlier introduced the phase factor $\exp\left(-\frac{\gamma_{nn}q^2}{2}\right)$ in $f_{NN}(q)$ by defining $a_{nn} = \beta_{nn} + i\gamma_{nn}$. Studies show that by treating γ_{nn} as a free parameter, good agreement between theoretical and experimental cross sections could be achieved [31–33]. Recently, considering three different models for the interaction potential, Dedonder et al. [34] have shown that the phase of the scattering amplitude is a sensitive function of the relative size of the radii of the real and imaginary parts of potential. Their study showed that unitarity forces a moderately accurate determination of the phase in standard amplitude analyses, but the *NN* analyses to date do not give the phase variation needed to achieve a good representation of the data in multiple scattering calculations. In spite of much work, no successful study of proton reaction cross section over a large energy range and using several forms of target nuclear density in addition to invoking some corrections to the Glauber model has been presented. In the present work, we keep the parameter β_{nn}, which is known as a slope parameter of *NN* elastic scattering differential cross section, as energy dependent while treating the phase parameter γ_{nn} as energy independent, its significance to reproduce the experimental data has been investigated.

The structure of the paper is as follows. Our approach is outlined in Section 2; more specifically, the Coulomb-modified Glauber model is applied to analyze proton total reaction cross sections for ^{12}C, ^{27}Al, ^{40}Ca, ^{56}Fe, and ^{208}Pb nuclei at the energies spanning 40–800 MeV. Three different forms of nucleon distribution in each nucleus have been considered and the results are compared with experimental data [6, 11] in Section 3. Except for p- ^{12}C and -^{27}Al, the reaction cross section predictions with Gambhir and Patil (GP) [35] semi-phenomenological target density agree fairly well with the data. The effect of Coulomb shift in proton beam energy has also been studied. We will also see that by introducing the phase parameter γ_{nn} in the $f_{NN}(q)$, the theoretical calculations of σ_R with GP density nicely reproduce the measured ones over the whole range of energy considered in this work. To substantiate our work, we have also calculated the elastic p-nucleus scattering cross sections at energy 295 MeV. Results show fairly good agreement with the experimental data. Finally, the concluding remarks are given in Section 4.

2 Mathematical Formalism

2.1 Glauber Approach for Reaction Cross-Section

In the Glauber model [15], the elastic scattering amplitude for the collision of a projectile nucleon with a target nucleus described by the ground state wave function Ψ_0 and of mass number A is written as

$$F_{el}(\boldsymbol{q}) = \frac{iK}{2\pi}\int d\boldsymbol{b}e^{i\boldsymbol{q}.\boldsymbol{b}}\left(1-e^{i\chi(\mathbf{b})}\right), \tag{1}$$

where K is the incident momentum of the projectile, q is the momentum transferred from the projectile to the target, and b is the impact parameter. The elastic differential scattering cross section is given by

$$\frac{d\sigma}{d\Omega} = |F_{el}(\boldsymbol{q})|^2, \tag{2}$$

and the total reaction cross section σ_R is calculated by

$$\sigma_R = \int_0^\infty d\boldsymbol{b}\left(1-\left|e^{i\chi(\boldsymbol{b})}\right|^2\right). \tag{3}$$

The optical phase shift-function $\chi(b)$, the key quantity in the Glauber theory, is related to the *NN* scattering operator by

$$e^{i\chi(\boldsymbol{b})} = \langle\Psi_0\left|\prod_{j=1}^{A}\left[1-\Gamma_{NN}\left(\boldsymbol{b}-\boldsymbol{s}_j\right)\right]\right|\Psi_0\rangle. \tag{4}$$

In the above Eq. (4), $\boldsymbol{s}_j$ is the two-dimensional coordinate of the *j-th* target nucleon relative to its center of mass, which lies

on the plane perpendicular to K, and $\Gamma_{\mathrm{NN}}(b)$ is the NN profile function.

The evaluation of $\chi(b)$, as seen from Eq. (3), requires multidimensional integration. In the multiple scattering descriptions of nuclear reactions at intermediate energies, situations often occur in which second and higher order corrections have to be calculated with some care [36]. On the other hand, their effects on the main contributions are usually small, and consequently, they hardly justify sophisticated and time-consuming computing. Therefore, it is often approximately evaluated in the optical limit approximation using the intrinsic normalized density $\rho(r)$ of the target nucleus, as follows:

$$e^{i\chi(\boldsymbol{b})} = exp\left[-A\int d\boldsymbol{r}\,\Gamma_{NN}(\boldsymbol{b}-\boldsymbol{s})\,\rho(\boldsymbol{r})\right]. \tag{5}$$

The profile function $\Gamma_{\mathrm{NN}}(b)$ is related to the NN scattering amplitude $f_{NN}(q)$ as:

$$\Gamma_{NN}(\boldsymbol{b}) = \frac{1}{2\pi ik}\int e^{-i\boldsymbol{q}\cdot\boldsymbol{b}} f_{NN}(\boldsymbol{q})d\boldsymbol{q}, \tag{6}$$

where k is the momentum of the projectile nucleon. It is well known that the Glauber theory is based on the high-energy small angle scattering approximations and the Gaussian parameterization of $f_{NN}(q)$ has been very successful in at least explaining the total reaction cross section experiments (which cross section is sensitive to the nuclear surface region.) Before applying it to the low-energy processes such as the one less than 100 MeV, its usefulness should be assessed carefully. We therefore treat the interactions of proton–proton and proton–neutron separately and take $f_{NN}(q)$ in the form:

$$f_{pi}(\boldsymbol{q}) = \frac{ik\sigma_{pi}}{4\pi}(1-i\alpha_{pi})e^{-a_{pi}\boldsymbol{q}^2/2}, \quad i = p(n) \tag{7}$$

where $\sigma_{pp}(\sigma_{pn})$ and $\alpha_{pp}(\alpha_{pn})$ are the pp (pn) total cross section and the ratio of the real to the imaginary parts of the forward scattering amplitude respectively. The parameter $a_{pi}=\beta_{pi}+i\gamma_{pi}$ with $\beta_{pp}(\beta_{pn})$ and $\gamma_{pp}(\gamma_{pn})$ are, respectively, slope parameters and the phase of the pp (pn) elastic scattering differential cross section. Using expression (7), Eq. (5) can be written as:

$$e^{i\chi(b)} = exp\left[\frac{iZ}{k}\int_0^\infty qdq\,J_0(qb)\,f_{pp}(q)\,F_p(q) + \frac{i(A-Z)}{k}\int_0^\infty qdq\,J_0(qb)\,f_{pn}(q)\,F_n(q)\right], \tag{8}$$

where $F_{p(n)}(q)$ is the form factor (Fourier transform) of the target proton(neutron) density.

Generally, to account for the deviation of projectile trajectory due to Coulomb field [18–20], the optical phase shift-function $\chi(b)$ is evaluated at b' instead of b where b' is the distance of the closest approach on the Coulomb trajectory of the target-projectile system and is related to b as:

$$b' = \xi + \sqrt{(\xi)^2 + b^2}, \tag{9}$$

where $\xi=\eta/k_{cm}$ with k_{cm} as the center of mass momentum, $\eta = \frac{Ze^2}{\hbar v}$ is the Sommerfeld parameter and v is the projectile nucleon velocity. By slightly reframing Eq. (9) as: $b^2 = b'^2-2b\xi \Rightarrow b \approx b'-\xi$, and therefore, using the expression for $e^{i\chi(b')}$ from Eq. (8), the total reaction cross-section σ_R is calculated numerically by

$$\sigma_R = 2\,\pi\int_{2\xi}^{\infty}(b'-\xi)db'\left(1-\left|e^{i\chi(b')}\right|^2\right) \tag{10}$$

and the elastic scattering amplitude $F_{el}(q)$ as

$$F_{el}(q) = F_c(q) + iK\int_{2\xi}^{\infty}(b'-\xi)db'J_0(qb')e^{i\chi_c(b')}\left(1-e^{i\chi(b')}\right). \tag{11}$$

In the above expression, $F_c(q)$ is the point Coulomb scattering amplitude and $\chi_c(b)$ is the point Coulomb phase shift.

2.2 Input for Glauber model

The two main inputs required to calculate σ_R in the Glauber model are: nucleon density distribution of the target nucleus and the NN scattering amplitude. As mentioned earlier, we use the target densities that distinguish between the neutron and proton distributions. So, in addition to known realistic target density as determined from electron/proton scattering experiments, two more different semi-phenomenological nucleon density models are considered in this work.

2.2.1 Folded Yukawa density

With assuming a Yukawa interaction for the nucleon–nucleon interaction in the double folding procedure to obtain a potential, one often expresses the densities of nuclei by a step function of range R convoluted with a Yukawa-smearing function of some finite range [37]. Broglia and Winther [37] have made a detailed study

for the number of nuclei by utilizing the folded-Yukawa density:

$$\rho_i(r) = \rho_i^0 \; \mathcal{F}(k_i, R_i); \quad i = p, n \tag{12}$$

that consists of two parts

$$\mathcal{F}(k,R) = \begin{cases} 1 - (1+kR)\,\dfrac{\sinh(kr)}{kr} e^{-kR} & for\ r < R \\ \left[R\,cosh(kr) - \dfrac{\sinh(kR)}{k}\right]\dfrac{e^{-kr}}{r} & for\ r \geq R \end{cases} \tag{13}$$

where the parameters are expressed as a function of the mass number A:

$$k_p = (1.65 + 0.2\,A^{-1/3})\,fm^{-1}; \qquad k_n = (1.16 + 1.0\,A^{-1/3})\,fm^{-1}$$

$$R_p = (1.20A^{1/3} - 0.26)\,fm; \qquad R_n = (1.20A^{1/3} - 0.43)\,fm$$

$$\rho_p^0 = \frac{Z}{A}\,0.14(1.0 + 0.65\,A^{-1/3})\,fm^{-3} \qquad \rho_n^0 = \frac{N}{A}\,0.14(1.0 + 1.08\,A^{-1/3})\,fm^{-3}$$

2.2.2 Gambhir and Patil density

The GP semi-phenomenological density [35] $\rho_{n(p)}(r)$ is defined as:

$$\rho_i(r) = \frac{\rho_i^0}{1 + \left[0.5\left(1 + \frac{r^2}{R^2}\right)\right]^{\alpha_i}\left(e^{\frac{(r-R)}{a_i}} + e^{\frac{-(r+R)}{a_i}}\right)}; \quad i = p, n \tag{14}$$

with

$$a_i = \frac{\hbar}{2\sqrt{2m\epsilon_i}} \tag{15}$$

and

$$\alpha_i = \frac{q}{\hbar}\sqrt{{}^{m}/_{2\epsilon_i}} + 1 \tag{16}$$

where ε_i is the separation energy of the last proton or neutron, m is the corresponding nucleon mass, and

$$q = \begin{cases} (z-1)e^2 & proton \\ 0 & neutron. \end{cases}$$

The expression (14) has three unknowns, namely, ρ_p^0, ρ_n^0, and R. The first two are determined from the normalization conditions for the proton and neutron densities. Thus, the GP density model has only one adjustable parameter R called half-density radius, which is the value of r at which the density falls to half of its central value to a good approximation. The parameter R is determined by requiring that the root mean square radius (*rmsr*) r_p of the proton density as given by the model should be the same as deduced from the experimental charge *rmsr* r_c of the nucleus after accounting for the charge *rmsr* of a proton. The GP density parameter values for the target nuclei considered in this work are given in Table 1.

Coming to the parameters of *NN* amplitude as defined by Eq. (7), we use the following parameterizations [19, 20] for σ_{pp} and σ_{pn} which reproduce the observed values in the energy range 10 to 1,000 MeV quite well:

$$\sigma_{pp} = 13.73 - 15.04\,v^{-1} + 8.7\,v^{-2} + 68.67\,v^4 \tag{17}$$

$$\sigma_{pn} = -70.67 - 18.18\,v^{-1} + 25.26\,v^{-2} + 113.85\,v, \tag{18}$$

where σ_{pp} and σ_{pn} are in mb. To calculate α_{pp} and α_{pn}, we use the parameterizations of Ahmad et al. [38]:

$$\alpha_{pp} = -0.386 + 1.224\,exp\left[-0.5\left(\frac{k-0.427}{0.178}\right)^2\right] + 1.01\,exp\left[-0.5\left(\frac{k-0.592}{0.638}\right)^2\right] \tag{19}$$

$$\alpha_{pn} = -0.666 + 1.437\,exp\left[-0.5\left(\frac{k-0.412}{0.196}\right)^2\right] + 0.617\,exp\left[-0.5\left(\frac{k-0.797}{0.291}\right)^2\right], \tag{20}$$

with k as is the incident nucleon lab momentum in GeV/c. The energy dependence of the parameters $\beta_{pp}(\beta_{pn})$ in the energy range 40 to 300 MeV is calculated from the following expression [30]:

$$\beta_{pi} = \frac{1 + \alpha_{pi}^2}{16\pi}\sigma_{pi} \tag{21}$$

and all the parameters needed for $f_{pi}(q)$ are quoted in Table 2. It should be noted that at energy above 300 MeV, because the pion production channel becomes open, the expression (21) is no longer applicable for the evaluation of β_{pi}. Furthermore, due to large uncertainty reported in the total elastic scattering data [39], we have taken the values of β_{pi} above 300 MeV from Ref. [2]. Finally, the phase parameter γ_{pi} is assumed to be free, and its significance is discussed in the next section.

3 Results and Discussion

Following the prescription outlined in Section 2, here, we show our numerical results for proton -^{12}C, -^{27}Al, -^{40}Ca, -^{56}Fe, and -^{208}Pb total reaction cross sections σ_R over the energies spanning 40–800 MeV and compare them with the measured experimental data. As already explained earlier, our main objective is to examine the effect of introducing the phase in the *pp* (*pn*) elastic scattering amplitude on proton-nucleus reaction cross section using three different nuclear densities for each target nucleus. Let us first study how accurate our theoretical results are considering various corrections but keeping phase parameters $\gamma_{pp}(\gamma_{pn})$ equal to zero, compared with the experimental σ_R data. The circles in Figs. 1, 2, 3.4, and 5 represents the experimental data compiled by Carlson et al. [6] whereas the data in triangles are taken from

Table 1 Parameter values of the GP semi-phenomenological density used in the calculation

A	Z	a_p (fm)	a_n (fm)	α_p	α_n	R (fm)
12	6	0.5702	0.526	1.198	1.0	2.145
27	13	0.792	0.630	1.660	1.0	2.714
40	20	0.789	0.575	2.041	1.0	3.496
56	26	0.712	0.68	2.230	1.0	4.070
90	40	0.789	0.658	3.132	1.0	4.776
208	82	0.805	0.8385	5.5244	1.0	6.632

Auce et al. [11]. In each figure, the dashed, dotted, and dot-dashed curves represent respectively, calculation of σ_R with GP [35], realistic and Folded Yukawa (FY) [37] densities. The realistic densities of ^{27}Al, ^{40}Ca, and ^{56}Fe nuclei have been taken from the tabulation of de Vries et al. [40] while for ^{12}C, the realistic nuclear form factor has been taken from Ahmad [41], and finally, for ^{208}Pb, we have used the parameterized nuclear form factors by Alvi et al. [42] obtained by fitting the form factors as given by the point proton and neutron densities by Ray et al. [43] in their analysis of 0.8 GeV polarized proton elastic differential cross section and analyzing power data. In Fig. 1, we compared the prediction of our calculations with measured p- ^{12}C reaction cross section data. As one can see from the figure, the dot-dashed curve, which is calculated using FY density agrees reasonably well with the measured one up to

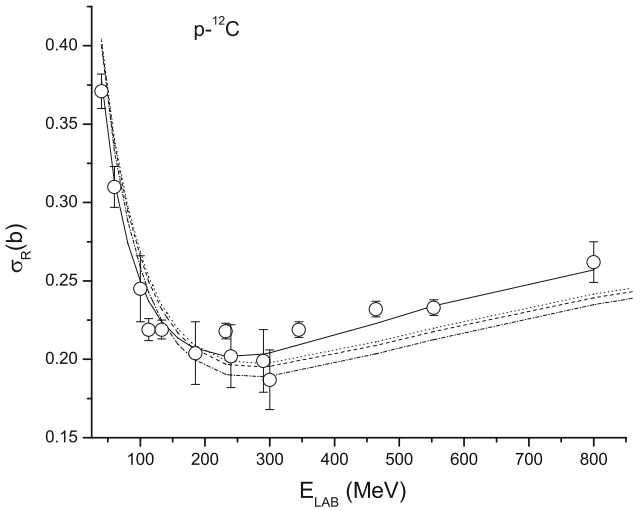

Fig. 1 Comparison of proton-^{12}C total reaction cross sections as a function of energy calculated with GP [35] density (*dashed curve*), realistic density (*dotted curve*) and FY [37] density (*dot-dashed curve*). *Full curve* represents σ_R by adding phase in the pp (pn) elastic scattering amplitude. The *circles* represent the experimental data taken from [6]

200 MeV than those calculated with other two densities. In fact, our result with FY density is almost the same as those of theoretical predictions reported in Ref. [11] up to energy 300 MeV obtained by Cooper et al. [12] using global potential EDAD fit 3 but better than microscopic calculation by Amos and

Table 2 Parameter values of the pp (pn) elastic scattering amplitude $f_{pi}(q)$ at different energies

Energy (MeV)	σ_{pp} (fm^2)	α_{pp}	β_{pp} (fm^2)	σ_{pn} (fm^2)	α_{pn}	β_{pn} (fm^2)
40	7.04	1.366	0.401	21.265	0.592	0.571
60	4.575	1.637	0.335	13.16	0.86	0.4555
81	3.423	1.786	0.285	9.27803	1.008	0.372
100	2.87	1.815	0.245	7.34	1.047	0.306
113	2.63	1.79	0.219	6.45	1.034	0.265
119	2.543	1.766	0. 208	6.126	1.019	0.248
133	2.39	1.694	0.184	5.506	0.967	0.212
141	2.326	1.643	0.1713	5.224	0.9296	0.194
158	2.231	1.521	0.1472	4.748	0.8366	0.1606
180	2.17	1.351	0.122	4.319	0.704	0.1285
185	2.163	1.313	0.117	4.24	0.673	0.122
232	2.185	0.989	0.086	3.767	0.407	0.087
240	2.2	0.943	0.0827	3.718	0.368	0.084
290	2.33	0.723	0.071	3.528	0.169	0.0722
300	2.37	0.691	0.0697	3.51	0.137	0.071
346	2.54	0.578	0.073	3.46	0.014	0.075
464	3.03	0.404	0.088	3.52	−0.225	0.077
553	3.39	0.294	0.11	3.62	−0.38	0.0859
700	3.94	0.119	0.16	3.807	−0.559	0.12
800	4.27	0.0115	0.185	3.922	−0.621	0.12
860	4.45	−0.0465	0.188	3.985	−0.64	0.13

Deb [13] as well as using global potential by Koning and Delaroche [14]. Above 200 MeV, σ_R curves calculated with GP and realistic densities give quantitatively good results.

For p- ^{27}Al results in Fig. 2, there is not much difference among the σ_R calculations using the mentioned three densities but above around 200 MeV, calculation with realistic density for target nucleus give good representation of the data. As there is no other theoretical study of energy dependence in the case of ^{27}Al, we are unable to compare the quality of our results presented here with any earlier analysis. Overall, our calculations agree reasonably well with the measured σ_R.

Figure 3 displays the result of σ_R for proton- ^{40}Ca nucleus. It is clear that the predictions of σ_R with GP density are close to the experimental data than calculated with the other two target densities. The dotted curve which represents our calculation using the realistic density, overestimates σ_R at high energies whereas the dot-dashed curve shows results with FY density, underestimates the proton reaction cross section at low energies. But in comparison with earlier works [11], our analyses with these densities provide better representation of measured data over the whole energy range. However, nearly similar results compared with our using GP density have been obtained by Amos and Deb [13].

In Figs. 4 and 5, we have illustrated the energy dependence of the proton reaction cross section for ^{56}Fe and ^{208}Pb nuclei. One can immediately observe that there is a drastic difference in quantitatively reproducing the data between the σ_R calculations with GP and that using the other two densities for target nuclei. In fact, using GP density, our theoretical calculation very nicely reproduces the data not only qualitatively but quantitatively as well over the whole range of energy. It should be mentioned that in Ref. [11], the data has been considered only up to 300 MeV and even then, their results show inferior agreement with experiment.

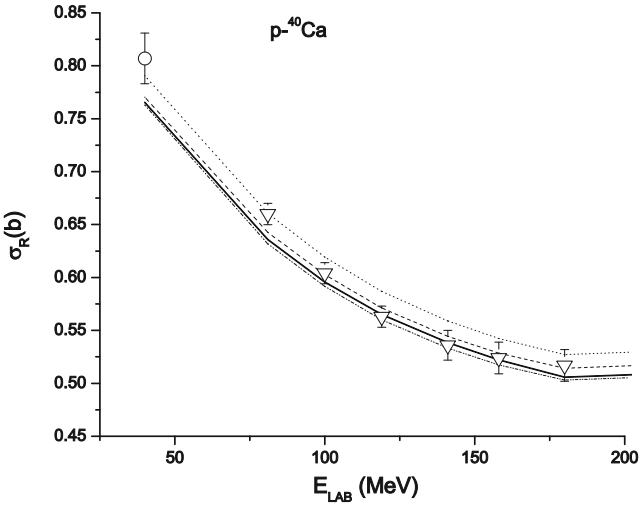

Fig. 3 Comparison of proton-^{40}Ca total reaction cross sections as a function of energy calculated with GP density (*dashed curve*), realistic density (*dotted curve*) and FY density (*dot-dashed curve*). The *circle* and *triangles* are the experimental data taken from [6, 11]

We have also accounted for in our calculations the Coulomb shift in energy of the proton as it enters the nuclear environment. In fact, due to the Coulomb field, when a charged projectile collides with a target nucleus, the effective kinetic energy of the projectile with which it undergoes nuclear interaction is different than the incident energy. Because a proton is positively charged, the shift in its energy is downward and so, the energy with which it interacts with the nucleon of the target nucleus is lower than given as the incident one. If $V_c(r)$ denotes the Coulomb potential energy between the projectile and the target nucleus, then the actual projectile energy E' is given as:

$$E' = E - V_c(r), \tag{22}$$

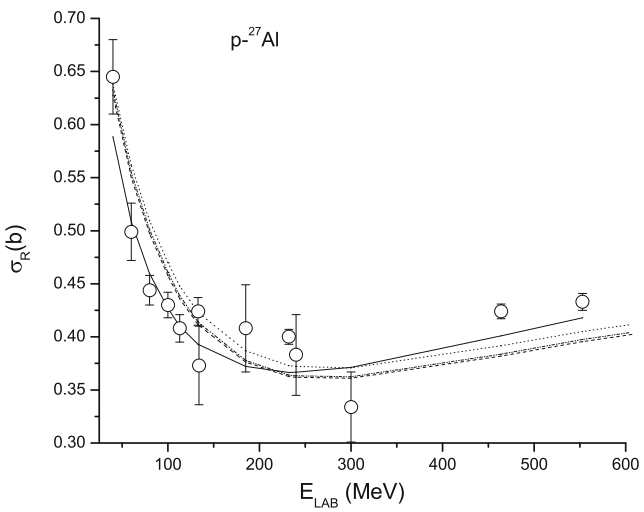

Fig. 2 Same as in Fig. 1 but for proton-^{27}Al total reaction cross sections

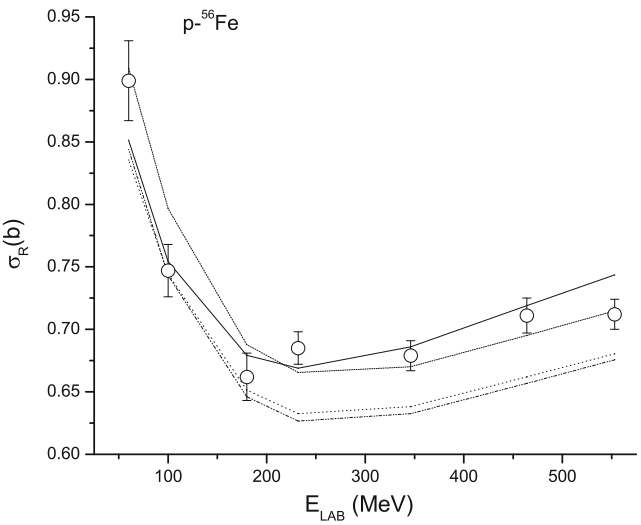

Fig. 4 Same as in Fig. 1 but for proton-^{56}Fe total reaction cross sections

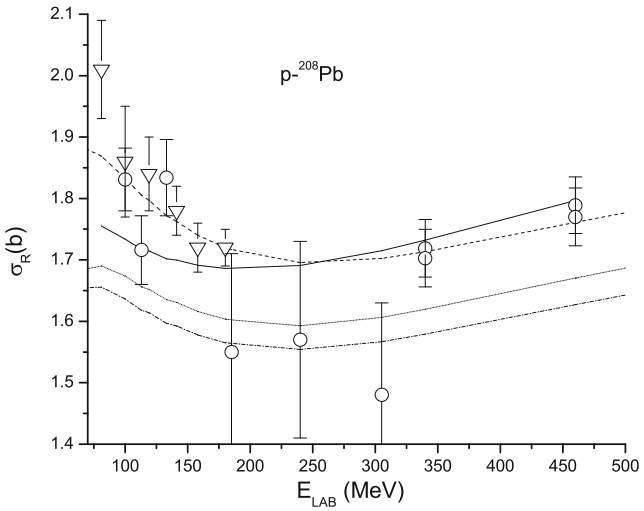

Fig. 5 Same as in Fig. 3 but for proton-^{208}Pb total reaction cross sections

with E as the given incident energy. Since $V_c(r)$ is r dependent, the calculation of energy E' is not an easy task in Glauber model. But as it is well known that the contribution to the reaction cross section comes mainly from the surface region, we approximate it as:

$$E' = E - V_c(R_{int}) \tag{23}$$

where the interaction radius R_{int} is related to experimental σ_R through the relation [19, 20]:

$$R_{int} = \sqrt{\frac{\sigma_R}{\pi}}. \tag{24}$$

The full curves in the figures represent the effect of introducing the phase $\gamma_{pp}(\gamma_{pn})$ in the pp (pn) elastic scattering amplitude Eq. (7). While keeping the value of $\gamma_{pp}(\gamma_{pn})$ equal to zero, it has already been seen from the figures that among all the three forms of the nuclear densities considered here, the GP density provides better representation of the data for most of the target nuclei. Neglecting medium effect, the phase parameter in NN scattering amplitude can depend on incident energy but must be independent of the target nucleus. Therefore, using GP phenomenological density, reaction cross section data for p- ^{12}C were fitted by varying the two phase

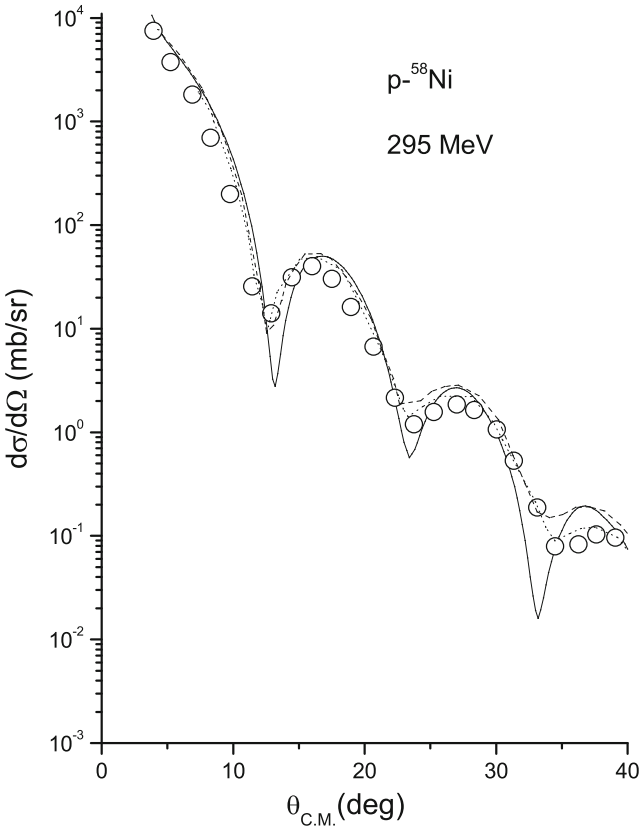

Fig. 6 Experimental data (*circles*) for proton-^{58}Ni elastic scattering differential cross sections at 295 MeV. *Full curve* represents our result using the GP density with γ_{pp}=0.614 and γ_{pn}=−0.763. *The dashed line* shows the result of the RIA calculations using RMF densities while the *dotted line* represents similar calculations but using densities deduced from electron scattering data [44]

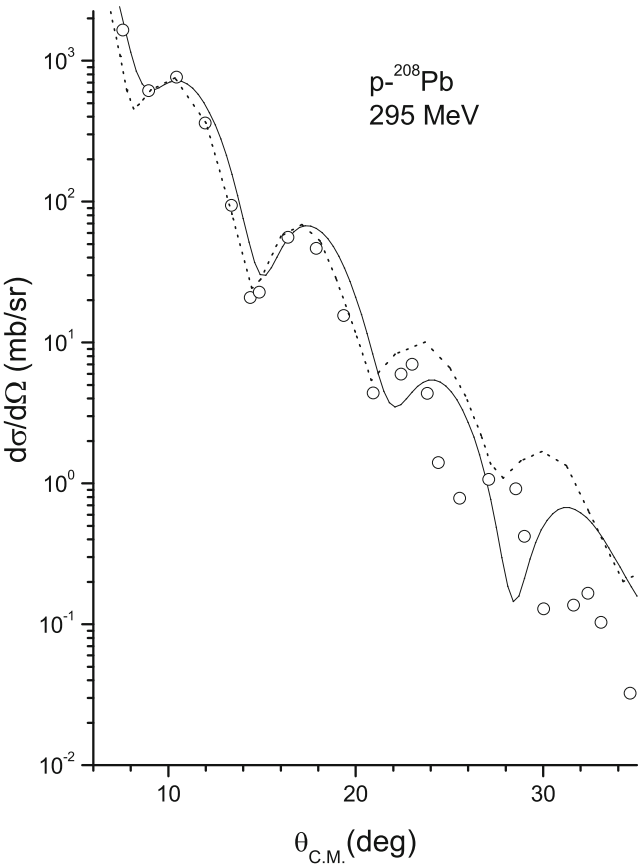

Fig. 7 Experimental data (*circles*) for proton-^{208}Pb elastic scattering differential cross sections at 295 MeV. *The solid line* represents our result using the GP density while the *dashed line* shows the result of medium-modified RIA calculation with Dirac–Hartree nucleon density [45]

parameters assumed to be energy independent as its dependence on energy is not established. The solid line in Fig. 1 shows the best fit to the σ_R data (χ^2 per point=1.4) with parameter values $\gamma_{pp}=0.614\pm0.256 fm^2$ and $\gamma_{pn}=-0.763\pm0.235 fm^2$. Next, we calculate the σ_R for ^{27}Al, ^{40}Ca, ^{56}Fe, and ^{208}Pb with the same values of $\gamma_{pp}(\gamma_{pn})$ as obtained in p-^{12}C fitting and the results are displayed with solid lines in Figs. 2, 3, 4, and 5. It is seen in the p-^{27}Al and ^{40}Ca reaction data that there is an excellent agreement over the whole range of energies considered in this work. For p-^{208}Pb, the result is not as good as with the GP density without considering the phase term in $f_{pi}(q)$ but it predicts better results compared with other two densities. For p-^{56}Fe, the parameter-free calculation agrees fairly well with experiment. The encouraging results of our approach emphasize the inclusion of phase in scattering amplitude at least in the calculation of total reaction cross sections.

Finally, in an attempt to affirm our work, we have calculated the elastic p-^{58}Ni and ^{208}Pb differential scattering cross section at 295 MeV. The solid line in Figs. 6 and 7 represent the optical limit result of p-^{58}Ni and p-^{208}Pb elastic scattering calculation using the GP density with *NN* parameters (average of 290 and 300 MeV) are taken from Table 2 whereas the $\gamma_{pp}=0.614 fm^2$ and $\gamma_{pn}=-0.763 fm^2$. The experimental data in circles are extracted from Ref. [44] and [45]. For comparison, we have also shown in Fig. 6 the results of the relativistic impulse approximation (RIA) calculations using relativistic mean field (RMF) densities (dashed line) and a similar calculation using densities deduced from electron scattering data (dotted line) [44]. In Fig. 7, the dashed line shows the result of medium-modified RIA calculation with Dirac–Hartree nucleon density [45]. It is seen that without varying the $\gamma_{pp}(\gamma_{pn})$ parameter of *NN* amplitude, that is using the values of $\gamma_{pp}(\gamma_{pn})$ obtained by fitting the p-^{12}C reaction cross section data, our calculation reproduces reasonably well the differential elastic scattering data at least in the forward direction where the Glauber model high-energy approximation is expected to work well.

4 Conclusion

Proton total reaction cross sections σ_R have been analyzed on ^{12}C, ^{27}Al, ^{40}Ca, ^{56}Fe, and ^{208}Pb over the beam energy spanning 40–800 MeV. Applying a Coulomb-modified Glauber model and using three types of the target densities with different proton and neutron distributions for each, we compare the theoretical predictions of σ_R with experimental data. Considering energy dependence in the slope parameter $\beta_{pp}(\beta_{pn})$ of *pp* (*pn*) elastic scattering amplitude $f_{pi}(q)$, our results show that except for the two low-mass nuclei ^{12}C and ^{27}Al, the predictions of σ_R with GP density reproduce reasonably well the experimental data for all other target nucleus. We have also accounted for the Coulomb shift in the beam energy. As expected, the inclusion of Coulomb shift is visible at low energies but we have not shown its effect in the figures.

In earlier works it has been discussed in details [28] that the energy dependence of slope parameters β_{NN} has little effect upon the calculation with eikonal approach of the Glauber model. To take this into account, we added an energy-independent phase parameter $\gamma_{pp}(\gamma_{pn})$ to $\beta_{pp}(\beta_{pn})$ and to our surprise, we found that its inclusion improves the theoretical values of σ_R and in one other case, it nearly reproduces the experimental data over the whole range of energy considered in this work. We hope that with the availability of some more proton reaction cross section data at intermediate energies for target nuclei our success will stimulate to study the energy dependence of phase parameter. Finally, in optical model calculations, the reaction cross section is sensitive to the amplitude of the scattered waves and not their phases but in the eikonal approach of Glauber model our results clearly demonstrate that the phase of the scattering amplitude does matter in the calculation of total reaction cross sections.

Acknowledgments The author is grateful to (late) Prof. I Ahmad who was his source of inspiration. The author would also like to acknowledge an anonymous BJPH reviewer for his/her carefully reviewing the paper and making suggestions that improved the quality of the manuscript. The author would also like to thank Prof. Ahmad A Al-Ghamdi for his encouragement during the course of this work.

References

1. O.A.P. Tavares, E.L. Medeiros, V. Morcelle, Physica Scripta **82**, 025201 (2010)
2. B. Abu-Ibrahim, W. Horiuchi, A. Kohama, Y. Suzuki, Physical Review **C 77**, 034607 (2008)
3. A. Shukla, B.K. Sharma, R. Chandra, P. Arumugam, S.K. Patra, Physical Review **C 76**, 034601 (2007)
4. A. Ozawa, Nuclear Physics A **738**, 38 (2004)
5. H.Y. Zhang et al., Nuclear Physics **A 707**, 303 (2002)
6. R.F. Carlson et al., Physical Review **C 49**, 3090 (1994)
7. S. Barshay et al., Physical Review **C 11**, 360 (1975)
8. L. Sihver, C.H. Tsao, R. Silberberg, T. Kanai, A.F. Barghouty, Physcal Review C **47**, 1225 (1993)
9. H.P. Wellisch, D. Axen, Physical Review **C 54**, 1329 (1996)
10. H.F. Arellano, M. Girod, Physics Review **C 76**, 034602 (2007)
11. A. Auce et al., Physics Review **C 71**, 064606 (2005)
12. E.D. Cooper, S. Hama, B.C. Clark, R.L. Mercer, Physics Review **C 47**, 297 (1993)
13. K. Amos, P.K. Deb, Physics Review **C 66**, 024604 (2002)
14. A.J. Koning, J.P. Delaroche, Nuclear Physics A **713**, 213 (2003)
15. R.J. Glauber, in *Lecture on Theoretical Physics vol. 1*, ed. by W.E. Brittin, L.C. Dunham (Interscience, New York, 1959), p. 315
16. J. Chauvin, D. Lebrun, A. Lounis, M. Buenerd, Physics Review **C 28**, 1970 (1983)
17. M. Buenerd, A. Lounis, J. Chauvin, D. Lebrun, P. Martin, G. Duhamel et al., Nuclear Physics A **424**, 313 (1984)
18. S.M. Lenzi, A. Vitturi, F. Zardi, Physical Review **C 40**, 2114 (1989)
19. S.K. Charagi, S.K. Gupta, Physical Review **C 41**, 1610 (1990)
20. S. K. Charagi, S. K Gupta Phys. Rev. C 46, 1982 (1992)
21. S. Prashant, Physical Review **C67**, 054607 (2003)
22. C. Deeksha, Z.A. Khan, Physical Review **C80**, 054601 (2009)

23. B. Abu Ibrahim, Y. Ogawa, Y. Suzuki, I. Tanihata, Computer Physics Communications **151**, 369 (2003)
24. I. Ahmad, M.A. Abdulmomen, J.H. Madani, Indian Journal of Physics **71A**, 61 (1997)
25. J.H. Madani, International Journal of Modern Physics **E 11**, 475 (2002)
26. M.A. Alvi, Nuclear Physics **A 789**, 73 (2007)
27. L. Ray, Physical Review **C 20**, 1857 (1979)
28. I. Ahmad, M.A. Abdulmomen, M.A. Alvi, International Journal of Modern Physics **E 11**, 519 (2002)
29. M.M.H. El-Gogary, A.S. Shalaby, M.Y.M. Hassan, A.M. Hegazy, Physical Review C **61**, 044604 (2000)
30. Y. Ogawa, K. Yabana, Y. Suzuki, Nuclear Physics **A543**, 722 (1992)
31. V. Franco, Y. Yin, Physical Review **C 34**, 608 (1986)
32. R.J. Lombard, J.P. Maillet, Physical Review **C 41**, 1348 (1990)
33. M.A. Hassan et al., Australian Journal of Physics **49**, 655 (1996)
34. J.P. Dedonder, W.R. Gibbs, M. Nuseirat, Physics Review **C 77**, 044003 (2008)
35. Y.K. Gambhir, S.H. Patil, Z. Physical A **324**, 9 (1986)
36. V. Franco, G.K. Varma, Physical Review **C 15**, 1375 (1977)
37. R.A. Broglia, A. Winther, *Heavy ion reactions: elastic and inelastic reactions, vol. 1* (Benjamin Cummings, Massachusetts, 1981), p. 172
38. I. Ahmad, M.A. Abdulmomen, L.A. Al-Khattabi, International Journal of Modern Physics **10**, 43 (2001)
39. W.M. Yao, Particle Data Group. Journal of Physics G: Nuclear and Particle Physics **33**, 1 (2006)
40. H. de Vries, C.W. de Jager, C. de Vries, Atomic Data and Nuclear **36**, 495 (1987)
41. I. Ahmad, Journal of Physics G: Nuclear and Particle Physics **6**, 947 (1980)
42. M.A. Alvi, M. Riyadh Arafah, F.S. Al-Hazmi, Journal of Physics G: Nuclear and Particle Physics **37**, 045101 (2010)
43. L. Ray, W.R. Coker, G.W. Hoffmann, Physical Review C **18**, 2641 (1978)
44. H. Sakaguchi et al., Physical Review **C 57**, 1749 (1998)
45. J. Zenihiro et al., Physical Review **C 82**, 044611 (2010)